Available online at www.sciencedirect.com
SCIENCE DIRECT®
Journal of Solid State Chemistry 178 (2005) 3471–3475
JOURNAL OF SOLID STATE CHEMISTRY
www.elsevier.com/locate/jssc

The crystal structure of $CuSb_2O_3Br$: Slabs from cubic Sb_2O_3 interspersed between puckered hexagonal CuBr-type layers

Zuzana Mayerová, Mats Johnsson*, Sven Lidin

Department of Inorganic Chemistry, Stockholm University, S-106 91 Stockholm, Sweden

Received 30 June 2005; received in revised form 31 August 2005; accepted 31 August 2005
Available online 3 October 2005

Abstract

The new compound $CuSb_2O_3Br$ crystallize in the monoclinic space group *Cc*. The unit cell parameters are $a = 7.9189(15)$ Å, $b = 13.7105(10)$ Å, $c = 19.048(2)$ Å, $\beta = 90^\circ$, $Z = 16$. The crystal structure is solved from single crystal data, $R = 0.0490$. The compound show a layered structure with slabs from cubic Sb_2O_3 interspersed in between puckered layers of CuBr. The Sb(III) atoms have tetrahedral [SbO_3E] coordination where E is the $5s^2$ lone pair, these units build up $Sb_4O_4E_6$ cages. The CuBr layers resemble those in hexagonal CuBr but the Cu(I) ions have actually tetrahedral [$CuBr_3O$] coordination. The Cu–O bonds link the Sb_4O_6 cages with the CuBr layers.

Keywords: Oxohalogenide; Stereochemically active lone pair; Sb_4O_6 cages; Layered crystal structure

1. Introduction

Elements with stereo chemically active lone pairs like Se^{4+}, Te^{4+} and Sb^{3+} are generally more chalcophilic than the late transition metals, and hence in quaternary compounds between lone pair elements, late transition metals, oxygen and halogens, there is a tendency for the transition metal to coordinate to halogen and for the lone pair element to coordinate directly to oxygen [1–3]. This leads to a subdivision of the structure into chalcogen/chalcophile and halogen/halophile parts. The inter-phase between these two regions is a non-bonding volume cohabited by the terminal halogens of the halophile substructure and the lone pairs of the chalcophile substructure. Although these relatively electron-rich entities would be expected to be mutually avoiding, they appear in the same subvolume in an overwhelming majority of the known examples, and the most plausible explanation for this behaviour is not the mutual attraction of lone pairs and halogens, but rather their concurrent expulsion from the bonding subvolume of the structure.

Sb^{3+} adopts two types of coordinations that both are frequent; one sided three coordination [SbO_3] and see-saw coordination [SbO_4]. The flexibility to accept both those types of coordination lead to that many oxide compounds containing Sb^{3+} show various types of antimony oxide entities arranged e.g. in form of small cages as in cubic Sb_2O_3 [4] or to form tubes as in $Sb_8O_{11}Cl_2$ [5].

In this article we present a compound with puckered hexagonal CuBr layers interspersed with Sb_4O_6 cages of the same type as found in cubic Sb_2O_3. The title compound is to our best knowledge the only oxohalogenide compound with Cu^+ in combination with Sb^{3+} except for $CuSbTeO_3Cl_2$ [2].

2. Experimental

Yellow single crystals of the new compound $CuSb_2O_3Br$ were obtained from chemical reactions in sealed evacuated silica tube. For the synthesis Sb_2O_3 (Aldrich, powder, $<5\,\mu m$, 99%), and CuBr (ABCR, min. 98%) were used as starting materials. The preparation was made from a stoichiometric mixture of Sb_2O_3:CuBr = 1:1 and subsequently heat treated in a Muffle furnace at 550 °C for 96 h. The synthesis product was a mixture of yellow–green

*Corresponding author. Fax: +46 8 15 21 87.
E-mail addresses: zuzana@inorg.su.se (Z. Mayerová), matsj@inorg.su.se (M. Johnsson), sven@inorg.su.se (S. Lidin).

0022-4596/$ - see front matter © 2005 Elsevier Inc. All rights reserved.
doi:10.1016/j.jssc.2005.08.028

powder and yellow $CuSb_2O_3Br$ single crystals. Chemical transport seems to take place during the synthesis as the single crystals were mainly found in one end of the silica tubes and could be physically removed. The isostructural compound $CuSb_2O_3Cl$ has also been synthesised with similar methods as the title compound and crystal structure data are deposited at the Fachinformationzentrum in Karlsruhe, see below.

Single-crystal X-ray data was collected on a STOE IPDS image-plate rotating anode diffractometer with use of graphite-monochromatized Mo$K\alpha$ radiation. The intensities of the reflections were integrated using the STOE software and absorption correction was carried out numerically, after crystal shape optimisation [6,7]. The structures were solved by direct methods (SHELXS97) [8] and refined by full matrix least squares on F using the program Jana2000 [9]. All atoms except for the oxygens were refined with anisotropic displacement parameters. The crystal data are reported in Table 1. All graphics are made with the program Diamond [10]. The chemical composition of the synthesis products were also confirmed in a scanning electron microscope (JEOL 820) equipped with an energy-dispersive spectrometer (LINK AN10000).

The monoclinic unit cell has been confirmed by X-ray powder diffraction using a 40 mm Guiner-Hägg focusing camera with subtraction geometry. Cu$K\alpha_1$ radiation ($\lambda = 1.54060$ Å) where used and silicon, $a = 5.430880(35)$ Å, was added as internal standard. The recorded films were read in an automatic film scanner and the data was evaluated using the programs SCANPI [11] and PIRUM [12].

Table 1
Crystal data for $CuSb_2O_3Br$

Empirical formula	$CuSb_2O_3Br$
Formula weight	434.9
Temperature	293(2) K
Wavelength	0.71073 Å
Crystal system	Monoclinic
Space group	$C1c1$ (no. 9)
Unit cell dimensions	$a = 7.9189(15)$ Å
	$b = 13.7105(10)$ Å
	$c = 19.048(2)$ Å
	$\beta = 90^\circ$
Volume	2068.0(5) Å^3
Z	16
Density (calculated)	5.5861 g cm^{-3}
Absorption coefficient	22.063 mm^{-1}
Absorption correction	Numerical
$F(000)$	3040
Crystal color	Yellow
Crystal habit	Hexagonal prism
Crystal size	$0.1 \times 0.1 \times 0.05$ mm^3
θ range for data collection	2.14–28.06°
Index ranges	$-10 \leqslant h \leqslant 10$
	$-18 \leqslant k \leqslant 18$
	$-24 \leqslant l \leqslant 24$
Reflections collected	7957
Independent reflections	4830 ($R_{int} = 0.0644$)
Completeness to $\theta = 28.06^\circ$	96.0%
Refinement method	Full-matrix least squares on F
Weighting scheme	$w = 1/[\sigma^2(F_o^2) + (0.0004F_o)^2]$
Data/restraints/parameters	4830/0/182
Goodness-of-fit on F	1.623
Final R indices [$I > 2\sigma(I)$]	$R = 0.0490$
	$wR = 0.0606$
R indices (all data)	$R = 0.0759$
	$wR = 0.0635$
Largest diff. peak and hole	5.81 and −2.82 (e Å^{-3})

3. Results and discussion

The new compound $CuSb_2O_3Br$ crystallizes in the monoclinic non-centro symmetric space group Cc, but pseudomerohedral mimetic twinning produces the Laue symmetry $6/mmm$. Structural solution was first attempted in the space-group $P6_3/mmc$, and the symmetry was then successively reduced to $P6_3mc$ and $Cmc2_1$. In the latter space group, a highly disordered solution could be found, but only after reducing the symmetry the disorder could be fully resolved in a twinned solution in the monoclinic space group Cc. The pair of twinning matrices produces: $-\frac{1}{2}-\frac{3}{2}$ 0, $-\frac{1}{2}\frac{3}{2}$ 0, the pseudo mimetic twinning observed: $\frac{1}{2}-\frac{1}{2}$ 0, $-\frac{1}{2}-\frac{1}{2}$ 0, in both compounds: 0 0 1, 0 0 1. The structural refinement gives that the relative volume of the parts of the twinned crystal are 0.200, 0.043, and 0.757, respectively. Experimental parameters, atomic coordinates and selected interatomic distances from the single crystal investigation are listed in Tables 1–3, respectively.

The monoclinic unit cell has been confirmed by powder X-ray diffraction that gives the following monoclinic C-centred cell: $a = 7.9909(59)$ Å, $b = 13.7544(73)$ Å, $c = 19.022(10)$ Å, $\beta = 90.00(6)^\circ$.

The crystal structure consists of puckered layers of CuBr with Sb_4O_6 clusters resembling those in cubic Sb_2O_3 interspersed between the layers, see Fig. 1. It is interesting to note that the two sub-motifs of the structure each allows a centre of symmetry; although the Sb_4O_6 cluster itself is non-centric, the arrangement of clusters would permit a centre of symmetry within that layer, at the centre of the hexagonal hole in that layer, at the approximate position $\frac{1}{4}, \frac{3}{4}, 0$. Similarly, the CuBr layer form a coloured 6^3 net that is non-centric, but the stacking allows for a centre of symmetry between the layers, at the positions corresponding to the nodes of the complementary 3^6 net, $\frac{1}{4}, \frac{11}{12}, 0$. In fact, the ideal position from the Sb_4O_6 layer instead coincides with the nodes of the 6^3 net. The relative stacking of the two layers thus precludes the presence of a centre of symmetry. There are eight crystallographically different Sb atoms. All these have a [SbO_3] trigonal pyramidal coordination of oxygen. If the $5s^2$ lone pair also is taken into consideration the coordination polyhedron becomes a [SbO_3E] tetrahedron. The [SbO_3E] groups build up two crystallographically different Sb_4O_6 cages that are of the same type as in cubic Sb_2O_3 [4]. Each cage thus consists of four [SbO_3E] groups that together form a supertetrahedron, see Fig. 2. In cubic Sb_2O_3, the Sb_4O_6 cages are

Table 2
Atomic coordinates and equivalent isotropic displacement parameters for $CuSb_2O_3Br$

Atom	x	y	Z	U_{eq}[a] [Å^2]	BVS[b]
Sb(1)	0.74350(1)	0.0821(2)	0.0772(1)	0.0130(7)	2.75
Sb(2)	0.9737(5)	0.3410(2)	0.0791(2)	0.0124(8)	2.82
Sb(3)	0.2434(5)	0.0692(2)	0.0801(2)	0.0131(7)	2.68
Sb(4)	0.5128(5)	0.3406(2)	0.0794(2)	0.0124(8)	2.90
Sb(5)	0.2434(5)	0.4297(2)	0.9200(2)	0.0129(7)	3.18
Sb(6)	0.5112(5)	0.1592(2)	0.9206(2)	0.0126(8)	3.02
Sb(7)	0.9751(5)	0.1587(2)	0.9212(2)	0.0121(8)	2.99
Sb(8)	0.74342(17)	0.41849(19)	0.92391(6)	0.0101(7)	2.90
Cu(1)	0.5137(6)	−0.0033(2)	0.2796(3)	0.0419(12)	1.13
Cu(2)	0.2446(7)	−0.2552(4)	0.7873(2)	0.0235(13)	1.11
Cu(3)	−0.2545(9)	−0.2562(4)	−0.2832(4)	0.0438(19)	1.28
Cu(4)	0.9731(6)	−0.0036(2)	−0.7201(3)	0.0410(12)	1.20
Br(1)	−0.0070(8)	−0.66573(13)	−0.2489(5)	0.0310(6)	1.01
Br(2)	0.4930(8)	−0.66547(13)	−0.2496(5)	0.0310(6)	1.06
Br(3)	0.7448(6)	−0.0868(3)	0.2247(3)	0.0199(12)	1.06
Br(4)	−0.7561(7)	−0.0893(3)	−0.7223(3)	0.0191(11)	1.01
O(1)	−0.946(2)	0.6504(12)	0.0229(11)	0.0116(6)	1.80
O(2)	−0.078(2)	0.1404(14)	−0.9782(11)	0.0116	2.08
O(3)	−0.574(2)	0.5207(14)	−0.0987(8)	0.0116	2.22
O(4)	−0.266(2)	−0.0436(14)	0.0198(10)	0.0116	1.92
O(5)	−0.943(2)	0.5211(13)	−0.0983(8)	0.0116	2.14
O(6)	−0.757(2)	0.7051(13)	−0.0985(7)	0.0116	2.11
O(7)	−0.447(2)	0.3510(13)	−0.0216(11)	0.0116	1.85
O(8)	0.924(2)	0.6396(12)	0.4789(11)	0.0116	2.10
O(9)	0.559(2)	0.5249(14)	0.6110(8)	0.0116	1.85
O(10)	0.234(2)	−0.0418(14)	0.4772(10)	0.0116	1.93
O(11)	0.922(2)	0.5251(13)	0.6117(8)	0.0116	1.89
O(12)	0.742(2)	0.7047(14)	0.6134(7)	0.0116	1.93

The Wyckoff positions for all atoms are 4*a*.
[a] $U_{(eq)}$ is defined as one-third of the trace of the orthogonalized U tensor.
[b] Constants for the bond valence sum (BVS) calculations are from [13,14].

arranged as separate clusters with only weak van der Waals interactions in between. An important difference in between those cages and these in the novel compounds is that the latter are not isolated; instead there are direct Cu–O bonds between the cages and the CuBr layers. The four crystallographically different Cu^+ ions in the CuBr layers have [$CuBr_3O$] tetrahedral coordination, see Fig. 3a,b.

The Sb–O distances varies in between 1.94 and 2.05 Å, the average bond length is 1.99 Å. The average Sb–O distance is thus longer compared to the value 1.977 Å for cubic Sb_2O_3 and can be understood from the presence of the Cu–O bonds in the present compounds. For one type of Sb_4O_6 cage three of the oxygens further bond to Cu^+ ions with Cu^+–O^{2-} distances of 2.242–2.361 Å. For the other type of cage there is only one Cu^+–O^{2-} bond (2.040 Å) and also two long Cu^+–O^{2-} interactions 3.293–3.301 Å that are too long to be considered as bond distances from bond valence sum calculations (BVS) according to Brown [13]. The average Cu^+–O^{2-} bond distance is 2.25 Å to be compared with 1.848 Å in Cu_2O [15]. The Sb_4O_6 cages are arranged in layers parallel to (110), see Fig. 4. The same kind of arrangement is observed for the (11-1) plane in cubic Sb_2O_3.

The CuBr layers resemble those in hexagonal CuBr [16,17], see Fig. 5. The Cu^+–Br distances are in between 2.382 and 2.473 Å (average 2.42 Å) that is to be compared with 2.365 Å in hexagonal CuBr. The Cu–Br distances are thus longer in the present compound compared to that in the triangular [$CuBr_3$] coordination in hexagonal CuBr due to the fact that Cu–O bonds also are present.

It is instructive to compare the compound to other intercalates. In graphite intercalates, the stacking sequence of the carbon layer is normally changed by the intercalation process to yield an A–A stacking. This is the case also for the title compound. CuBr itself that shows an A–B–A type stacking, but in the intercalate [CuBr][Sb_2O_3] the CuBr layers are stacked A–A–A (disregarding colouring). The interactions between the host and the guest are, however, uncommonly strong in the title compound. Normal graphite intercalates do not exhibit any distortion of the graphene layers, the only exception being the compound CF_{1-x} in which the graphene layers are believed to be extensively puckered, indicating a transformation from sp^2 to sp^3 carbon in accordance with the poor electrical conductivity of the compound. Intercalating donors, such as alkali metals, certainly transfer partial charge to the graphite network, but at the relatively low

Table 3
Bond lengths (Å) for $CuSb_2O_3Br$

Sb(1)–O(1)^{I}	2.047(19)
Sb(1)–O(2)^{ii}	1.939(20)
Sb(1)–O(4)^{iii}	2.042(19)
Sb(2)–O(8)^{iv}	1.97(2)
Sb(2)–O(11)^{iv}	1.981(18)
Sb(2)–O(12)^{iv}	2.043(17)
Sb(3)–O(9)^{v}	2.034(18)
Sb(3)–O(10)^{vi}	2.00(2)
Sb(3)–O(11)^{v}	2.010(17)
Sb(4)–O(7)^{iii}	1.96(2)
Sb(4)–O(9)^{iv}	1.974(19)
Sb(4)–O(12)^{iv}	2.028(17)
Sb(5)–O(3)^{ii}	1.944(18)
Sb(5)–O(4)^{vii}	1.94(2)
Sb(5)–O(5)^{ii}	1.970(17)
Sb(6)–O(1)^{viii}	1.98(2)
Sb(6)–O(5)^{viii}	1.961(18)
Sb(6)–O(6)^{viii}	1.972(17)
Sb(7)–O(2)^{ix}	1.98(2)
Sb(7)–O(3)^{viii}	1.969(19)
Sb(7)–O(6)^{viii}	1.984(17)
Sb(8)–O(7)^{ii}	2.05(2)
Sb(8)–O(8)^{x}	1.941(19)
Sb(8)–O(10)^{xi}	1.973(20)
Cu(1)–O(5)^{xii}	2.361(16)
Cu(1)–O(11)^{v}	3.293(15)
Cu(1)–Br(1)^{xiii}	2.386(4)
Cu(1)–Br(3)	2.399(7)
Cu(1)–Br(4)^{ii}	2.440(7)
Cu(2)–O(6)^{xiv}	2.242(15)
Cu(2)–Br(1)^{vii}	2.418(8)
Cu(2)–Br(2)^{xv}	2.445(8)
Cu(2)–Br(3)^{xvi}	2.473(7)
Cu(3)–O(12)^{xvii}	2.040(15)
Cu(3)–Br(1)^{xviii}	2.443(9)
Cu(3)–Br(2)^{xviii}	2.409(9)
Cu(3)–Br(4)^{xiii}	2.415(8)
Cu(4)–O(3)^{xix}	2.355(16)
Cu(4)–O(9)^{xx}	3.301(16)
Cu(4)–Br(2)^{xxi}	2.390(4)
Cu(4)–Br(3)^{xxii}	2.382(7)
Cu(4)–Br(4)^{xxiii}	2.445(7)

Symmetry codes: (i) $1.5+x, -0.5+y, z$; (ii) $1+x, y, 1+z$; (iii) $1+x, y, z$; (iv) $x, 1-y, -0.5+z$; (v) $-0.5+x, 0.5-y, -0.5+z$; (vi) $x, -y, -0.5+z$; (vii) $0.5+x, 0.5+y, 1+z$; (viii) $1.5+x, -0.5+y, 1+z$; (ix) $1+x, y, 2+z$; (x) $x, 1-y, 0.5+z$; (xi) $0.5+x, 0.5-y, 0.5+z$; (xii) $1.5+x, 0.5-y, 0.5+z$; (xiii) $0.5+x, -0.5-y, 0.5+z$; (xiv) $1+x, -1+y, 1+z$; (xv) $-0.5+x, 0.5+y, 1+z$; (xvi) $-0.5+x, -0.5-y, 0.5+z$; (xvii) $-1+x, -1+y, -1+z$; (xviii) $-0.5+x, 0.5+y, z$; (xix) $1.5+x, 0.5-y, -0.5+z$; (xx) $0.5+x, 0.5-y, -1.5+z$; (xxi) $0.5+x, -0.5-y, -0.5+z$; (xxii) $x, y, -1+z$; (xxiii) $2+x, y, z$.

concentrations, the limiting case being C_8K, graphite remains a metal. In contrast, the CuBr layers are electron-precise Cu^+ entities, and as the intercalation may be considered as an acid–base reaction between the

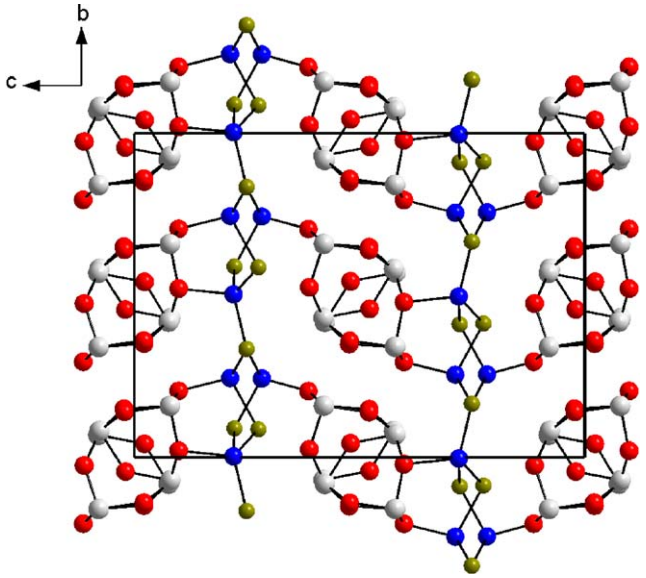

Fig. 1. Overview of the crystal structure for $CuSb_2O_3Br$ seen along [100]. The structure is built up by layers of Sb_2O_3 and layers of CuBr. Cu (blue), Br (green), Sb (grey), O (red).

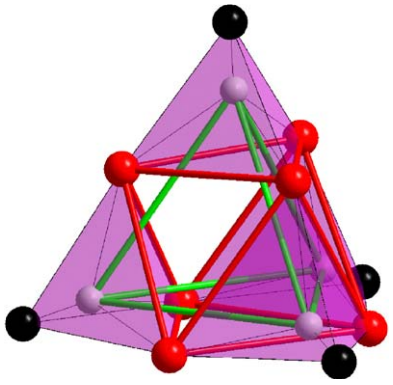

Fig. 2. The Sb_4O_6 cage is a supertetrahedron of four $[SbO_3E]$ tetrahedra (pink). The oxygens are arranged to form an octahedron and the antimony atoms to form a tetrahedron.

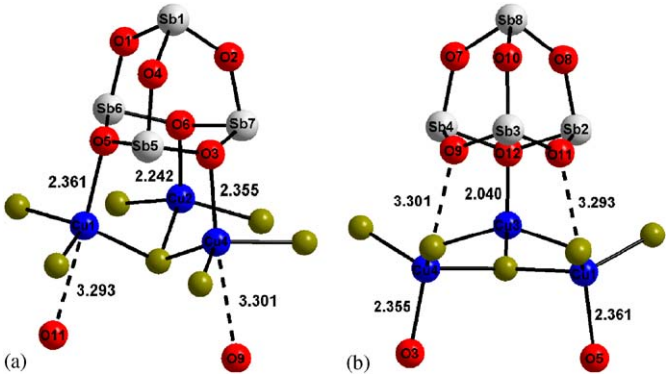

Fig. 3. There are two crystallographically different Sb_4O_6 cages with different relations to the CuBr layers in the crystal structures. The two types of Sb_4O_6 cages are connected to a CuBr layer by; (a) three Cu–O bonds, (b) One Cu–O bond.

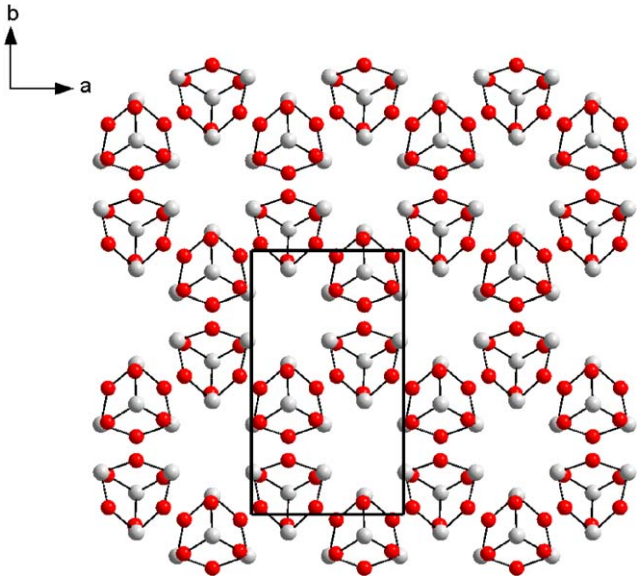

Fig. 4. The Sb_4O_6 cages are arranged as slabs from cubic Sb_2O_3, view along [001].

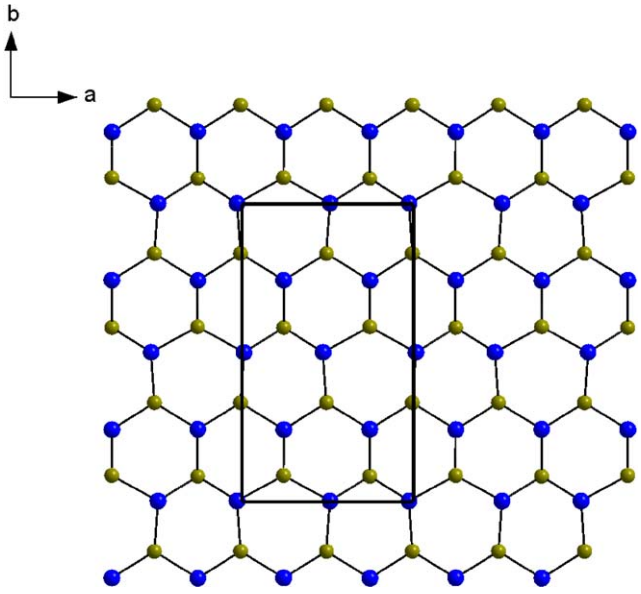

Fig. 5. A puckered CuBr layer seen along [001]. The arrangement is almost hexagonal, but the puckering breaks this symmetry.

electron rich Sb_2O_3 donor and the electron poor Cu acceptor, it is accompanied by a relatively large structural adjustment to yield tetrahedrally coordinated Cu.

4. Conclusion

The new layered compound $CuSb_2O_3Br$ is synthesised in a sealed evacuated silica tube starting with Sb_2O_3:CuBr in the stoichiometric molar ratio 1:1. The compound crystallizes in the non-centrosymmetric monoclinic space group *Cc*, the crystal structure is solved from single crystal data with a twin model. There are Sb_4O_6 cages resembling those in cubic Sb_2O_3, but they are not isolated clusters instead there are Cu–O bonds linking them with CuBr layers. The CuBr layers bear similarities to the layers in hexagonal CuBr but they are puckered due to the Cu–O bonds. The fact that there is Cu–O bonds present in between the Sb_4O_6 cages and the CuBr layers causes the bonding distances in between Cu–O, Cu–Br and Sb–O to be longer compared to in the compounds Cu_2O, hexagonal CuBr and cubic Sb_2O_3.

5. Supplementary material

Supplementary Material has been sent to Fachinformationzentrum Karlsruhe, Abt. PROKA, 76344 Eggenstein-Leopoldshafen, Germany (fax: +49-7247-808-666; E-mail: crysdata@fiz-karlsruhe.de), and can be obtained on quoting the deposit numbers CSD-415539 for $CuSb_2O_3Br$ and CSD-415540 for $CuSb_2O_3Cl$.

Acknowledgment

This work has been carried out through financial support from the European Union (HPHN-CT-2002-00193) and the Swedish Research Council.

Appendix A. Supplementary materials

Supplementary data associated with this article can be found in the online version at doi:10.1016/j.jssc.2005.08.028.

References

[1] T.F. Semenova, I.V. Rozhdestvenskaya, S.K. Filatov, L.P. Vergasova, Miner. Mag. 56 (1992) 241–245.
[2] R. Becker, M. Johnsson, R.K. Kremer, P. Lemmens, Solid State Sci. 5 (2003) 1411–1416.
[3] M. Johnsson, S. Lidin, K.W. Törnroos, H.-B. Bürgi, P. Millet, Angew. Chem, Int. Ed. 43 (2004) 4292–4295.
[4] C. Svensson, Acta Cryst. B 31 (1975) 2016–2018.
[5] F. Sgarlata, Period. Mineral. 39 (1970) 315–328.
[6] X-RED, Version 1.07, STOE & Cie GmbH, Darmstadt, Germany, 1996.
[7] X-SHAPE revision 1.09, STOE & Cie GmbH, Darmstadt, Germany, 1997.
[8] G.-M. Sheldrick, SHELXS-97—Program for the solution of Crystal Structures, Göttingen, 1997.
[9] V. Petříček, M. Dusek, Institute of Physics AVCR, Praha, Czech Republic, 2000.
[10] K. Brandenburg, DIAMOND Release 2.1e, Crystal Impact GbR, Bonn, Germany, 2000.
[11] K.E. Johansson, T. Palm, P.E. Werner, J. Phys. Sci. Instrum. 13 (1980) 1289–1291.
[12] P.E. Werner, Ark Kemi. 31 (1969) 513–516.
[13] I.D. Brown, D. Altermatt, Acta Cryst. B 41 (1985) 244–247.
[14] R. Restori, D. Schwarzenbach, Acta Cryst. B 42 (1986) 201–208.
[15] G.P. Shields, P.R. Raithby, F.H. Allen, W.D.S. Motherewell, Acta Cryst. B 56 (2000) 455–465.
[16] J. Krug, L. Sieg, Z. Naturforsch., Teil A 7 (1952) 369–371.
[17] W. Buehrer, W. Haelg, Electrochim. Acta 22 (1977) 701–704.